The role of metal–organic frameworks in a carbon-neutral energy cycle

Alexander Schoedel[1,2,3], Zhe Ji[1,2,3] and Omar M. Yaghi[1,2,3,4]*

Reducing society's reliance on fossil fuels presents one of the most pressing energy and environmental challenges facing our planet. Hydrogen, methane and carbon dioxide, which are some of the smallest and simplest molecules known, may lie at the centre of solving this problem through realization of a carbon-neutral energy cycle. Potentially, this could be achieved through the deployment of hydrogen as the fuel of the long term, methane as a transitional fuel, and carbon dioxide capture and sequestration as the urgent response to ongoing climate change. Here we detail strategies and technologies developed to overcome the difficulties encountered in the capture, storage, delivery and conversion of these gas molecules. In particular, we focus on metal–organic frameworks in which metal oxide 'hubs' are linked with organic 'struts' to make materials of ultrahigh porosity, which provide a basis for addressing this challenge through materials design on the molecular level.

Around 86% of all energy used globally comes from burning fossil fuels[1], generating 35 billion tons of carbon dioxide annually[2]. The continuing reliance on fossil fuels by developed countries[3] and the increasing demand for energy by emerging countries[4] make the emission of carbon dioxide into the atmosphere a serious global problem. This has provided impetus for finding alternative energy from solar, wind, geothermal, hydropower, biomass and nuclear fission sources. Although these are active areas of research and development, and are being used in some countries, they still constitute a minority of the global energy supply because of various issues related to cost, storage, scalability and safety[5]. It is widely believed that we will continue to be reliant on fossil fuels for the foreseeable future[6] and so it is urgent in the short term to address carbon dioxide emissions, while continuing to develop alternative fuels as a long-term solution (Fig. 1).

In this Review, we examine the use of metal–organic frameworks (MOFs; Box 1) in the development of a carbon-neutral energy cycle involving the use of hydrogen as a long-term objective, methane as a transitional fuel with lower carbon dioxide emission than petroleum and the capture of carbon dioxide as an immediate solution. Specifically, we outline the progress in using MOFs to: store hydrogen, which is the ultimate fuel because it burns cleanly and produces only water as a by-product; store and deliver methane for use in automobile fueling; and capture carbon dioxide from flue gas in power plants and potentially other combustion sources (Fig. 1). We also include recent results on the emerging field of using MOFs and related frameworks not only to capture, but also to convert carbon dioxide to high-value chemicals. For each of the three gases (hydrogen, methane and carbon dioxide), we present the various means of their production, and the potential and limitations of the technologies and materials being pursued for their capture, storage and utilization. A running theme of this Review pertains to how the flexibility with which MOFs can be designed, assembled and precisely modified on the atomic and molecular levels provides unparalleled opportunities for solving these problems and ultimately achieving a carbon-neutral energy cycle.

Hydrogen production and storage technologies

Hydrogen is widely used in oil refining, methanol and ammonia synthesis, metal treatment and food production. The amount of hydrogen produced annually in the USA is equivalent to more than 1% of the total primary energy consumption[7]. In addition to its use as an industrial chemical, hydrogen is considered a clean energy carrier for a sustainable energy future, where it could be used in the conversion of energy from renewable sources, such as solar and wind, to electricity and work at the point of end use, producing only water as the by-product. Assuming the least carbon-intensive hydrogen production process and a high level of fuel cell vehicle market penetration, carbon dioxide emissions from light-duty vehicles could be reduced to 36.2% of the expected level by 2050[7]. This corresponds to only 706 million metric tons annually, compared with the expected level, without use of hydrogen, of 1,950 million metric tons. Besides the application in fuel cell vehicles, stationary power applications such as back-up and distributed power supply systems (powering light equipment) are also envisaged as a part of the future hydrogen economy.

To satisfy the demand for hydrogen in the emerging markets, advanced technologies that produce hydrogen at lower cost, approximately by a factor of four, should be developed to compete economically with the present fossil fuel technology[7]. Traditional production methods of hydrogen including steam methane reforming and coal gasification, provide hydrogen supply at a cost of US$1.21–1.47 kg^{-1} (ref. 8). However, to facilitate an overall clean energy cycle, the emission of carbon dioxide as the by-product of these processes needs to be mitigated through carbon capture and sequestration. Biomass gasification currently offers comparable pricing at US$1.44 kg^{-1} with less carbon dioxide emitted, but it is impractical for large-scale production because of land requirements. Another route to generate hydrogen from renewable energy sources is to split water by electrochemical, photo-electrochemical and thermochemical processes. Instead of using carbon-emitting electricity grids, such electrolysis technologies powered by dedicated renewable sources, however, suffer from high cost, ranging from US$3.82–7.26 kg^{-1}, and low conversion efficiency[9]. Apart from the cost-prohibitive production, challenges in transportation, distribution and storage of hydrogen are more critical constraints in the deployment of a hydrogen economy; aspects we discuss below. In view of these issues, replacing currently dominant fossil fuels with hydrogen is still far from being widely practised.

[1]Department of Chemistry, University of California, Berkeley, California 94720, USA. [2]Materials Sciences Division, Lawrence Berkeley National Laboratory, Berkeley, California 94720, USA. [3]Kavli Energy Nanoscience Institute, University of California, Berkeley, California 94720, USA. [4]King Abdulaziz City for Science and Technology, PO Box 6086, Riyadh 11442, Saudi Arabia. *e-mail: yaghi@berkeley.edu
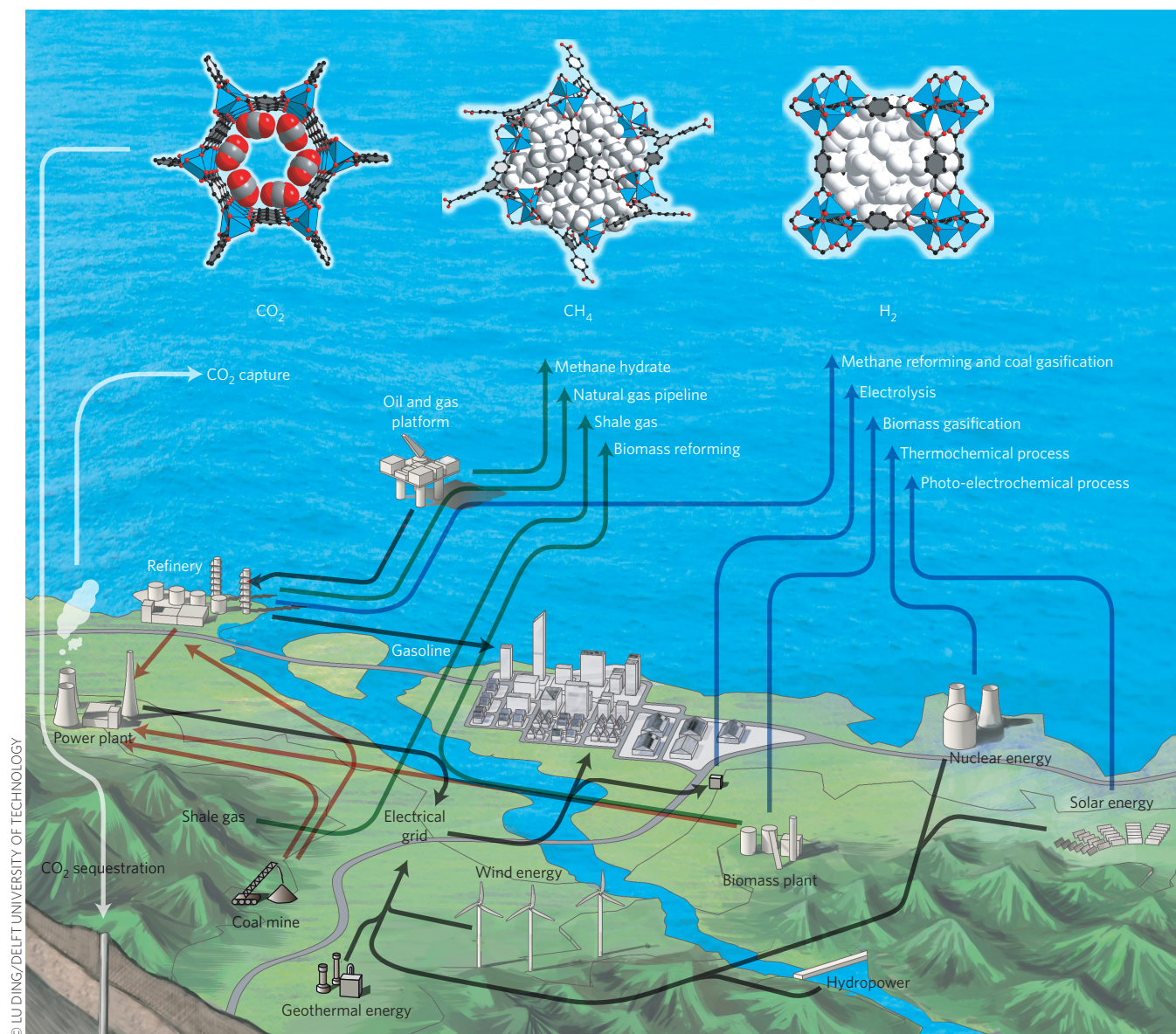
Figure 1 | Production pathways of key gases in the provision of energy. Coloured arrows represent the flow of different energy carriers or by-products: green, methane; blue, hydrogen; red, traditional fuels with high carbon content; black, electricity; white, carbon dioxide.

Conventional hydrogen storage applications and challenges. Hydrogen storage may be used in both stationary and transportation applications. In contrast to stationary storage systems, which can be large and operate at high pressures and temperatures, storage systems for use in vehicles must have the minimum possible weight and volume, to enable a reasonable driving range. Therefore, such systems are far more challenging to develop, and specific materials requirements include low weight, low volume, low cost and high durability, in addition to a very low heat transfer for charge/recharge cycles[8].

Current hydrogen storage technologies operate under relatively high pressure between 5,000 and 10,000 psi (350 to 700 bar), with an energy content of 4.4 MJ l^{-1}, using tanks made of carbon fibre-reinforced composite materials. Such energy densities are still marginal when compared with gasoline (31.6 MJ l^{-1}) and their cost is extremely high (a factor of 100 greater than gasoline). The use of liquid hydrogen, with an energy content of 8.4 MJ l^{-1}, is also hampered because of considerable safety issues and the high cost of liquefaction at −253 °C. Solid-state storage is mainly concerned with metal hydrides and complex hydride materials, such as sodium borohydride, which liberate hydrogen on heating. Metal hydrides, such as $PdH_{0.6}$ or rare earth (RE) hydrides of formula REH_2 or REH_3, are not suitable for on-board storage under conditions of 0–100 °C and 1–10 bar (ref. 10). Intermetallic compounds (such as $LiNi_5$) have problems including maximum uptakes of around 2 wt% or nonreversible hydrogen uptake ($Li_3Be_2H_7$, 9 wt%) in the required temperature and pressure range. In addition, there is a considerable cost argument associated with such alloys, given the fact that high-purity metals are expensive and subject to market fluctuations. Lightweight borohydrides or alanates can absorb up to 18 wt% hydrogen, but the reversibility of the reaction is strongly dependent on the particular system and operation temperatures usually range from 80 to 600 °C.

The biggest challenge in today's hydrogen economy is the considerable gap between its associated costs in comparison to fossil fuels. Creating new rather than developing existing technologies might overcome these obstacles. The Fuel Cells Technology Office of the US Department of Energy (DOE) has therefore set targets to develop such new technologies towards practical utility, including

Box 1 | Definitions and chemical structures.

MOFs are composed of metal oxide units stitched together covalently by organic linkers to make architecturally stable extended structures supporting permanent porosity. As shown in the figure, both inorganic and organic constituents of MOFs can be varied in their shape, size, composition, geometry and branching modality to produce a versatile class of porous crystalline solids[95]. Thus, the pore shape and size are designed nearly at will to produce MOFs with ultrahigh porosity (greater than 7,000 $m^2 g^{-1}$ internal BET surface area) and pore sizes up to 98 $Å$[74]. The rigidity and strong bonding within and to the metal oxide units (referred to as SBUs) has led to a large number of MOFs having high architectural, thermal and chemical stability[96]. These characteristics have allowed their covalent functionalization, whereby their interior pore space (shown here by the yellow sphere) is modified by carrying out reactions on the organic linkers and open metal sites. These modifications span the gamut of organic reactions, coordination of ligands to open metal sites and metallation of the organic linkers. The precision with which MOFs can be made and modified, coupled with the preservation of their high crystallinity after modification, has motivated their study in many applications such as gas adsorption, selective separations, catalysis and imaging, to mention a few examples[97]. The term MOF was introduced in 1995[98] and the number attached is roughly the chronological order of discovery. Other terms are used to name MOFs, often using an abbreviation of the place of discovery (for example, HKUST) or a structural feature (for example, PCN), followed by a number.

The constituents of MOFs. The schematic shows the structures of some SBUs and organic linkers used in MOFs. The empty pore space (yellow sphere) can be further modified through covalent functionalization. Colour code: grey, C; red, O; dark grey, Cl; blue, metal. Hydrogen atoms are omitted for clarity.

Table 1 | Current benchmark MOFs for cryogenic (77 K) hydrogen storage at high pressures.

Material	Formula [AU: ok?]	BET area ($m^2 g^{-1}$)	Capacity (wt%)	Pressure (bar)
MOF-210[24]	$(Zn_4O)_3(BTE)_4(BPDC)_3$	6,240	15.0	80
DUT-32[25]	$(Zn_4O)_3(BTCTB)_4(BPDC)_3$	6,411	14.2	80
NU-100[31]	$Cu_3(L^1)$	6,143	14.1	70
MOF-200[24]	$Zn_4O(BBC)_2$	4,530	14.0	80
NU-111[32]	$Cu_3(L^2)$	5,000	11.9	110
MOF-205[24]	$(Zn_4O)_3(BTB)_4(NDC)_3$	4,460	10.7	80
MOF-177[22]	$Zn_4O(BTB)_2$	4,500	9.9	70
SNU-77H[94]	$Zn_4O(TCBPA)_2$	3,670	9.9	90

H_3BTE, 4,4',4''-(benzene-1,3,5-triyl-tris(ethyne-2,1-diyl))tribenzoic acid; H_2BPDC, biphenyl-4,4'-dicarboxylic acid; H_3BTCTB, 4,4',4''-(benzene-1,3,5-triyltris(carbonylimino))tris-benzoic acid; H_6L^1, 5,5',5''-(((benzene-1,3,5-triyltris(ethyne-2,1-diyl))tris(benzene-4,1-diyl))tris(ethyne-2,1-diyl))triisophthalic acid; H_3BBC, 4,4',4''-(benzene-1,3,5-triyl-tris(benzene-4,1-diyl))tribenzoic acid; H_6L^2, 5,5',5''-(benzene-1,3,5-triyltris(buta-1,3-diyne-4,1-diyl))triisophthalic acid; H_3BTB, 4,4',4''-benzene-1,3,5-triyl-tribenzoic acid; H_2NDC, 2,6-naphthalenedicarboxylic acid; H_3TCBPA, tris(4'-carboxybiphenyl)amine; SNU, Seoul National University.

various cost, performance and safety requirements[11]. In addition to the overall vehicle performance, a reasonable refuelling time and a minimum driving range of 300 miles, there are other specific targets that need to be met by 2020. These targets comprise an energy capacity on a mass basis of 1.8 kWh kg^{-1} system (equivalent to 5.5 wt% hydrogen uptake) and on a volume basis of 1.3 kWh l^{-1} system (0.040 kg H_2 l^{-1}), in addition to a cost target of US$10 per kWh (US$333 kg^{-1} stored hydrogen capacity). This translates to a volumetric capacity of 40 g l^{-1} — a capacity that is currently reached in second-generation vehicles at 10,000 psi (for comparison: liquid hydrogen at −253 °C contains 71 g l^{-1}). The operating conditions are further limited to temperatures of −40 to 60 °C (that is, full exposure to direct sunlight) and pressures of below 100 atm (approximately 1,500 psi)[12].

MOFs for hydrogen storage. Hydrogen storage in MOFs has gained popularity since automobile manufacturers such as Mercedes-Benz[13] and Ford, together with BASF and the University of Michigan[14], announced a programme to utilize high-surface-area MOFs as storage media in future hydrogen tanks for vehicular applications. In addition, the US DOE continues to undertake considerable efforts and create funding opportunities towards the development of high-performance hydrogen storage materials.

Scientific efforts have been made to develop and modify MOFs for hydrogen storage. However, we would like to note that cryogenic (77 K) conditions at ambient pressure (1 bar) are impractical, simply because of the relatively low uptake capacity achieved. The benchmark MOF with such a capacity is based on the $Cu_2(-COO)_4$ paddlewheel secondary building units (SBUs; Box 1), termed PCN-12 (PCN, porous coordination network), with a total uptake of 3.05 wt% (23.2 g l^{-1}) at 77 K (ref. 15).

As suggested by the US DOE, hydrogen storage materials filled in tanks may operate at pressures of up to 100 atm and as low as −40 °C. However, most high-pressure studies in MOFs were conducted at 77 K, owing to the fact that hydrogen–framework interactions, typically van der Waals, are usually weak and decrease at higher temperatures[16]. Additionally, the introduction of open metal sites (OMSs) can boost the hydrogen storage performance of MOFs, especially at lower pressures, as they provide strong binding sites for the hydrogen molecules[17]. In this context, the higher the OMS density, the higher the hydrogen uptake; however, the alignment of OMSs with respect to each other — for example, in a close packing — can also play a critical role in cooperatively enhancing hydrogen–framework interactions[15]. Small pore sizes that closely fit the hydrogen molecule and therefore provide a greater overlapping potential have also been shown to increase the hydrogen affinity/capacity. These narrow pockets can be achieved either by introducing shorter linkers or by framework catenation[18]. Other successful

strategies are the incorporation of alkaline or alkaline-earth metal ions (Li$^+$, Mg^{2+})[19], or the doping of MOFs with metal nanoparticles to generate sites for hydrogen spillover[20]. However, some of the best performing MOFs, for high-pressure cryogenic hydrogen storage, have ultrahigh surface areas and are summarized in Table 1. For practical storage and delivery purposes, the total uptake is more relevant than the excess uptake, which is the measurable quantity. The capacity (in wt%) is calculated according to wt% = (mass of H_2)/(mass of MOF + mass of H_2) × 100% (some literature values show higher wt% because the mass of hydrogen is neglected in the denominator).

The quest for high-surface-area MOFs started in 2004, when we reported a strategy for the synthesis of highly porous frameworks and made MOF-177[21], which is until today one of the best hydrogen storage materials in terms of gravimetric uptake (110 mg g^{-1}; 9.9 wt%)[22]. This structure was obtained by linking octahedral $Zn_4O(-COO)_6$ SBUs together with a triangular BTB (H_3BTB: 4,4',4''-benzene-1,3,5-triyl-tribenzoic acid) linker into a framework with a net topology that inherently precludes interpenetration. Interpenetration usually occurs in MOFs with simple topology or low connectivity and is mostly counterproductive in the generation of high surface areas[23]. MOF-177 shows a Brunauer–Emmett–Teller (BET) surface area of 4,500 $m^2 g^{-1}$ and was subjected to isoreticular expansion in 2010 to afford MOF-200 (4,530 $m^2 g^{-1}$)[24]. Hydrogen sorption measurements at 77 K and 80 bar revealed an overall uptake of 163 mg g^{-1} (14.0 wt%). At present, $Zn_4O(-COO)_6$ units are frequently used to produce high-porosity MOFs, and the use of mixed linkers with this SBU is especially feasible and has generated many structures, for example, MOF-210 and DUT-32[25] (DUT, Dresden University of Technology). Combination of a linear (H_2BPDC: biphenyl-4,4'-dicarboxylic acid) and a triangular (H_3BTE: 4,4',4''-(benzene-1,3,5-triyl-tris(ethyne-2,1-diyl))tribenzoic acid) linker enabled the synthesis of highly porous MOF-210 (Fig. 2). At the time of its synthesis, this material held the world record in BET area with a value of 6,240 $m^2 g^{-1}$, and the highest gravimetric hydrogen storage capacity at 80 bar (176 mg g^{-1}, 15.0 wt%)[24].

Another design strategy to obtain high surface area MOFs is the use of high-connectivity building blocks as exemplified by metal–organic polyhedra (MOP-1)[26,27]. These design and synthetic approaches emerged as early as 2008[28] and recently led to ultrahigh-surface-area MOFs such as NOTT-116[29], PCN-68[30], NU-100[31] and NU-111[32] (NOTT, University of Nottingham; NU, Northwestern University), all of which are based on the same topology and have open metal sites at the Cu-paddlewheels. NU-100 and NU-111 are special in this context, as they not only show BET surface areas of 6,143 and 5,000 $m^2 g^{-1}$, respectively, but also rank among the best materials for cryogenic hydrogen storage with respective uptake capacities of 14.1 and 11.9 wt%.
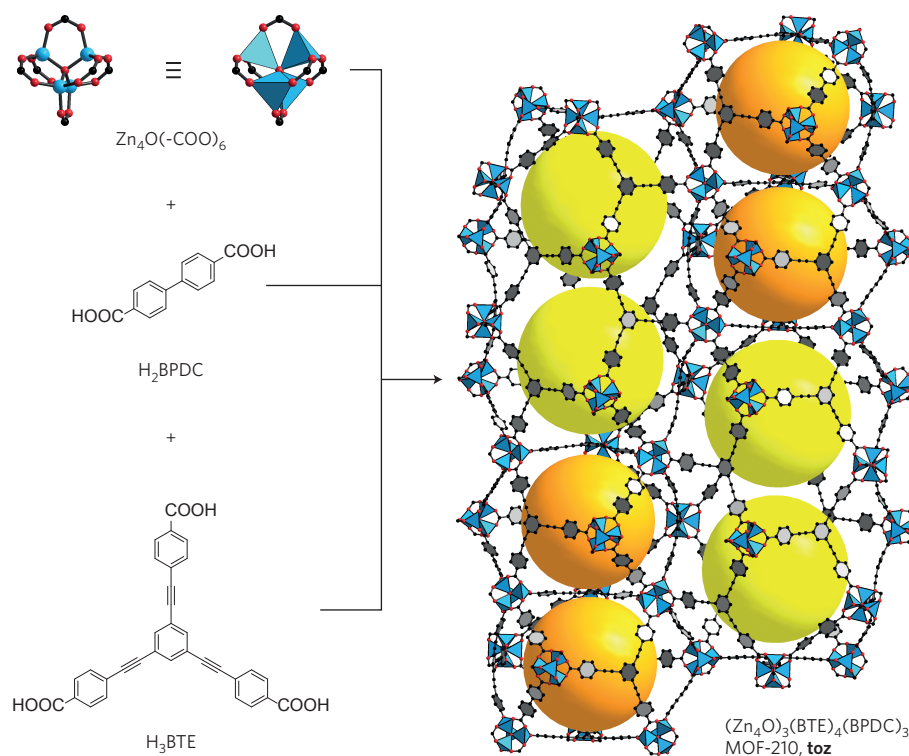
Figure 2 | Crystal structure of MOF-210. The benchmark material displays an ultrahigh surface area of 6,240 m² g⁻¹ and a H₂ uptake of 15.0 wt% (80 bar, 77 K). The spheres represent the largest molecules, which could fit in the pore without touching the van der Waals surface of the framework atoms. The different colours of the spheres indicate structurally different pores. Hydrogen atoms are omitted for clarity. Colour code: black, C; red, O; blue, Zn. H₃BTE, 4,4′,4″-(benzene-1,3,5-triyl-tris(ethyne-2,1-diyl))tribenzoic acid; H₂BPDC, biphenyl-4,4′-dicarboxylic acid.

The properties of the above-mentioned MOFs emphasize the importance of ultrahigh surface area as a critical design element for new hydrogen storage materials. To that end, it was recently suggested that by using computational methods, a maximum gravimetric surface area of 14,600 m² g⁻¹ can be theoretically obtained through systematic linker elongation[33]. However, we would like to emphasize that although longer linkers lead to higher surface areas, they also require more complicated synthetic procedures and thus have higher cost. The solution to this problem might be the incorporation of multiple geometrically different linkers to achieve higher structurally ordered complexity, as exemplified in MOF-210[34–36].

Theoretical efforts have also been made to address hydrogen storage in MOFs. Regimes that were identified by conducting grand canonical Monte Carlo (GCMC) simulations on a series of isoreticular MOFs (IRMOFs) revealed that the amount of adsorbed gas correlates with the heat of adsorption at low pressures, with surface area at medium pressures and with the pore volume at high pressures[37]. It was also confirmed through GCMC simulations and density functional theory (DFT) calculations that strong adsorption sites, such as open metal sites, are favourable at low pressures[38]. An optimal heat of adsorption for achieving appreciable hydrogen storage capacity at room temperature was estimated to be in the range of 18.5–22 kJ mol⁻¹. Thus far, heats of adsorption of up to 15.1 kJ mol⁻¹ have been achieved through the use of strong open metal sites[39]. In addition, the importance of high surface areas rather than large pore volumes was computationally validated[40].

In view of the current US DOE targets for hydrogen storage, considerable effort would be required to raise the storage temperature to at least −40 °C from −196 °C. Besides all considerations that encompass the design, synthesis and intrinsic properties of MOFs, there are also materials processing considerations needed for practical utility. Such key requirements include moisture stability, thermal conductivity and low cost[41].

Methane production and storage technologies

Methane, the main component of natural gas, contains much less carbon per unit of energy than any other fossil fuel. Thus, natural gas-fuelled vehicles emit 270 g of carbon dioxide per mile driven compared with 450 g of carbon dioxide emitted per mile from conventional gasoline[42]. Accordingly, methane can serve as a wide-scale transitional fuel for the foreseeable future before the advent of the hydrogen economy, especially when considering the already well-established pipeline infrastructure in many countries, including the USA and China. In comparison to 1,200 miles of hydrogen pipelines, there are 295,000 miles of natural gas transmission lines and 1.9 million miles of natural gas distribution lines in the USA, delivering approximately 23 trillion cubic feet of natural gas every year. The availability of methane is further supported by a substantial increase in natural gas reserves during recent decades, accessible through advanced technologies for exploiting unconventional methane sources, such as shale gas, methane hydrate, biomass reforming and underground coal gasification. Nowadays, the price of natural gas is 57% lower than gasoline on an energy-equivalent basis, reaching a historically low point. However, even at an attractive price relative to gasoline, methane constitutes only a 2% share of the US transportation market. One economic barrier arises from the limited number of methane refuelling stations. At-home gas refuelling might be a solution in this context, but the installation cost would need to be lowered by a factor of four to achieve a five-year payback. More importantly, the 70% lower volumetric energy density of methane compared with gasoline when compressed to 250 bar represents another fundamental challenge, making sorbent materials of high demand to facilitate methane on-board storage with high capacity.

Methane storage technologies and US DOE targets. Similar to hydrogen, methane storage is also focused on either transportation

Table 2 | MOFs for methane storage and delivery.

Material	Formula	Volumetric uptake (cm³ cm⁻³)	Volumetric delivery (cm³ cm⁻³)	Gravimetric uptake (g g⁻¹)	Gravimetric delivery (g g⁻¹)
HKUST-1[43]	$Cu_3(BTC)_2$	267*	190	0.216	0.154
MOF-519[49]	$Al_8(OH)_8(BTB)_4(H_2BTB)_4$	259	210*	0.194	0.157
Al-**soc**-MOF-1[50]	$(Al_3O)_2(TCPT)_3$	197	176	0.415*	0.371*

Uptake measured at a pressure of 65 bar and delivery at 5–65 bar. All measurements taken at 298 K. *Current benchmark values.

or stationary applications, the latter being especially important in view of vehicle home-refuelling applications. As detailed above, the lower average carbon dioxide emission for natural gas in comparison to gasoline makes it an environmentally and economically attractive target as a transitional technology. Up to 90% of today's natural gas vehicles operate with a low-cost steel tank that contains methane in the form of compressed natural gas (CNG). However, CNG at 250 bar (3,600 psi) is currently 30% less effective than gasoline and therefore its low energy density needs to be addressed in future storage technologies. Liquid natural gas has a higher energy density (22.2 MJ l⁻¹) than CNG (9.2 MJ l⁻¹) but there is a considerable energy/cost argument associated with liquefaction at −162 °C.

Recently, the Advanced Research Projects Agency-Energy (ARPA-E) of the US DOE has initiated a new programme titled 'Methane Opportunities for Vehicular Energy'[42]. The newly set targets for methane on-board storage systems are gravimetric capacities of 0.5 g$_{(methane)}$ g⁻¹$_{(sorbent)}$ or 700 cm³$_{(methane)}$ g⁻¹$_{(sorbent)}$ at 298 K and 65 bar. Such pressure is considered practically relevant as it can be reached by inexpensive two-stage compressors[43]. The gravimetric target then translates to a volumetric capacity of 263 cm³ (standard temperature and pressure, STP) cm⁻³ when the density of methane ($\rho = 0.188$ g cm⁻³ at 250 bar) is used as a reference. It is suggested that a 25% packing loss, due to pelletization, should be included in the calculations, which brings the initial volumetric capacity up to 330 cm³ (STP) cm⁻³. These ambitious new targets have recently been controversially discussed with respect to economic competition versus practical realization, particularly in view of the targeted volumetric working capacity (315 cm³ (STP) cm⁻³)[44]. For automobile fuelling applications, the working capacity — that is, the usable amount of methane in a tank — is of great current interest and more important than the total uptake. According to technical specifications, 3–5 bar of methane pressure needs to remain unused in the fuel tank, which leads to a usable methane delivery between maximum adsorption operational pressure (usually 65 or even 80 bar) and this set lower limit. In this context, a high methane affinity at low pressures adversely affects the materials performance towards practical utility, even if the overall uptake is high.

MOFs for methane storage and delivery. Methane storage in MOFs has recently regained momentum in comparison to the already established fields of carbon capture and hydrogen storage, but began in earnest in 2002, when we explored a series of robust IRMOFs towards high methane uptake[45]. Such frameworks represent expanded and/or functionalized derivatives of MOF-5[46], in which surface area and methane capacity could be systematically varied. In this context, a hydrophobic, C_2H_4-functionalized variant, IRMOF-6, showed the highest gravimetric (205 cm³ (STP) g⁻¹) and volumetric uptake (155 cm³ (STP) cm⁻³ (36 atm, 298 K)) at that time, exceeding all conventional porous materials by far. Other materials, such as $Cu(BPY)_2SiF_6$ (BPY, 4,4′-bipyridine) that are based on single metal nodes were also investigated towards methane storage and show gravimetric uptake capacities of 146 cm³ (STP) g⁻¹ at 298 K and 36 atm[47].

As the US DOE initiated a new methane storage programme in 2012, with the targets as described above, several research groups are actively developing and evaluating MOFs for methane storage under practically relevant conditions. In this context, a prototypical MOF termed HKUST-1 (HKUST, Hong Kong University of Science and Technology) that is a well-known and extensively studied material composed of $Cu_2(-COO)_4$ paddlewheel SBUs and BTC linkers (H₃BTC, 1,3,5-benzenetricarboxylic acid) was recently suggested to be used as a benchmark for the development of new methane storage materials[43,48]. HKUST-1 has a BET surface area of around 1,800 m² g⁻¹ and a volumetric methane capacity of 267 cm³ cm⁻³, which meets the current US DOE target, if potential packing losses are neglected (Table 2). Its working capacity — the amount of methane adsorbed between 65 and 5 bar — is 190 cm³ cm⁻³. For comparison, the working capacity of a tank without MOF filling is 62 cm³ cm⁻³. Another advantage of HKUST-1 is its commercial availability as Basolite C300 by BASF. Our laboratory has recently developed aluminium MOFs, termed MOF-519 and MOF-520, which are composed of $Al_8(OH)_8(-COO)_{16}$ SBUs joined together by triangular BTB linkers[49]. MOF-519 is special in this context, as it contains partially uncoordinated BTB linkers, narrowing pore space in comparison to MOF-520 (Fig. 3). It shows a BET surface area of 2,400 m² g⁻¹ and can adsorb 259 cm³ cm⁻³ methane with an exceptional deliverable capacity of 210 cm³ cm⁻³ at 65 bar and 298 K.

A very recently reported aluminium MOF with ultrahigh surface area (BET, 5,585 m² g⁻¹) has set new benchmarks in terms of gravimetric uptake and gravimetric working capacity[50]. Al-**soc**-MOF-1 is composed of a trigonal prismatic $Al_3O(-COO)_6$ SBU that, when combined with TCPT (H₄TCPT, 3,3′′,5,5′′tetrakis(4′carboxyphenyl)-*p*-terphenyl), affords a material that shows a total methane uptake of 0.42 g g⁻¹ and a deliverable capacity of 0.37 g g⁻¹ at 65 bar or 5–65 bar and 298 K, respectively. This material reached the gravimetric US DOE target of 0.5 g g⁻¹, albeit at 288 K and 80 bar. However, none of these materials can meet the current ARPA-E target for working capacity of 315 cm³ cm⁻³, which also includes packing loss after pelletization. Modelling studies suggest that these targets cannot be met with current technologies, as the energy density is set at 25% higher than CNG[44]. This is a potential growth area for post-synthetically modified MOFs.

There are several critical design elements in MOF chemistry to target high volumetric and gravimetric uptake, and working capacity. The high-performance materials with respect to gravimetric uptake/delivery usually display ultrahigh surface areas, as exemplified by Al-**soc**-MOF-1, NU-111[32], NU-125[51] and MOF-205[24]. A trend can be observed that high surface area together with mesopores shows a lower gravimetric uptake than high-surface-area microporous MOFs. In contrast, smaller pore sizes and the occurrence of open metal sites might be useful to reach high volumetric uptakes, as exemplified by HKUST-1 and Ni-MOF-74[52]. The high volumetric working capacity of MOF-519 most likely arises from the confined pore space provided by partially uncoordinated BTB moieties plus the absence of open metal sites, which usually represent primary adsorption sites, occupied at pressures below 5 bar. These examples clearly demonstrate that MOFs are superior to conventional materials with respect to methane storage, as they can be rationally fine-tuned to address specific targets.
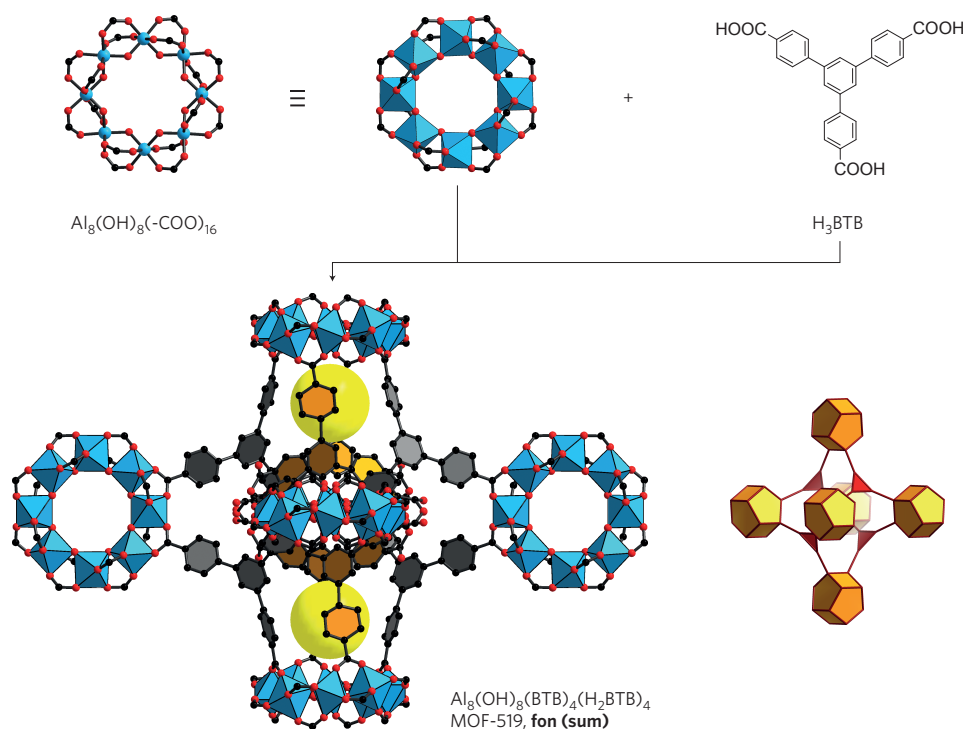
Figure 3 | Crystal structure of MOF-519. The material is composed of $Al_8(OH)_8(-COO)_{16}$ SBUs and BTB linkers. The linkers highlighted in grey are part of the extended framework; the ones in orange are protruding into the pores. Hydrogen atoms are omitted for clarity. Colour code: black, C; red, O; blue, Al. The spheres represent the largest molecules, which could fit in the pore without touching the van der Waals surface of the framework atoms. H_3BTB, 4,4′,4″-benzene-1,3,5-triyl-tribenzoic acid.

The recent computational work on MOFs for methane storage has gained popularity, as it can considerably aid experimental efforts by predicting the features of an ideal material. Here, large-scale screening of more than 130,000 MOFs, using known building blocks and their joining with different partially hypothetical linkers, has led to materials with higher predicted performance than the synthesized ones, at pressures of up to 35 bar[53]. This study revealed important parameters, such as an optimal surface area of 2,500–3,000 m^2 g^{-1}, a void fraction of around 0.8, the beneficial effect of methyl-, ethyl- and t-butyl-groups, and ideal pore diameters in the range of 4–8 Å. A more recent 'materials genome' strategy addressed the new ARPA-E targets, particularly the 315 cm^3 cm^{-3} deliverable capacity[44]. It was highlighted, by studying more than 650,000 structures, including but not limited to MOFs, that none of the materials approaches the current target, with only a few of them surpassing a value of 188 cm^3 cm^{-3}. The ongoing challenge was therefore identified as having a material with an optimal pore diameter of around 11 Å, a large number of adsorption sites and a low density.

Carbon dioxide capture and conversion

The concentration of atmospheric carbon dioxide has risen sharply from the preindustrial level of 280 parts per million (ppm) to more than 400 ppm in 2015[54,55] and therefore the stabilization goal, which was set to hold the global average temperature below 2 °C above pre-industrial levels (corresponding to a carbon dioxide level of 450 ppm) at the 2015 United Nations Climate Change Conference to avoid severe climate change, is rapidly approaching[56]. As a carbon-neutral economy may remain elusive for years, an urgent response is required to mitigate the environmental impact of the combustion of carbon-based fuels. To switch carbon dioxide emissions from an exponential trajectory to a flat path, at least eight wedges (a wedge is defined as a set of activities, such as substituting natural gas for coal, more efficient cars and the use of wind power, among others) have to be accomplished where each represents an activity that reduces

cumulatively 100 billion tons of carbon dioxide emission over the next 50 years[57]. This goal could be achieved with currently available technologies or just simple lifestyle changes, such as reduced reliance on cars, substituting natural gas for coal, and the capture and storage of carbon dioxide from power plants, among others. In the long term, stabilization of the atmospheric carbon dioxide concentration eventually requires the net emissions to drop to zero through revolutionary technologies.

Research into carbon dioxide capture and sequestration can contribute both to satisfying the urgent need to reduce carbon dioxide emissions and facilitating the ultimate carbon-neutral economy in the future. Capture is most effective when large quantities of carbon dioxide are generated on site, for example in power stations and methane-reforming plants. Technologies currently under development are capable of capturing carbon dioxide from post-combustion flue gas mixtures with carbon dioxide concentrations of around 12–14% (ref. 6). In addition to post-combustion flue gas, pre-combustion and oxy-combustion capture are other options for concentrated carbon dioxide capture to achieve higher efficiency. Pre-combustion strategies capture carbon dioxide from gasification mixtures of fuels before the combustion process, generating hydrogen that is delivered and consumed at sites of end use without any further release of carbon dioxide into the atmosphere. Oxy-combustion employs relatively pure oxygen instead of air for combustion to obtain concentrated carbon dioxide. After carbon dioxide is selectively captured, the second step is to sequestrate and store it in subsurface geologic formations, at 100–150 bar in depleted oil and gas fields at around 800–1,000 m below the surface[58], where no release into the atmosphere can occur over a relatively long period of time. So far, the most challenging step is the carbon dioxide capture, which requires selective and rapid processes with minimal energy input (Box 2).

MOFs for selective carbon dioxide capture. In recent years, extensive scientific efforts have been made in developing MOFs to address

Box 2 | State-of-the-art carbon capture.

One of the biggest challenges in the capture of carbon dioxide is the presence of moisture in flue gas streams emitted from power plants and other combustion sources. Attempts to address this matter have led to the emergence of different technologies, but ultimate solutions to this fundamental problem are yet to be discovered. State-of-the-art capture technologies are mainly based on liquid or solid adsorbents as well as membranes. Liquid adsorbents are nowadays broadly applicable for carbon dioxide separation as they are well developed, easy to handle, relatively inexpensive and exhibit high gas solubility and selectivity[99]. In this context, amines have been widely studied, the most popular examples being MEA solutions[100]. In such technologies, carbon dioxide is adsorbed from flue gas at nearly ambient temperature (mostly 40 °C) and the amine solution is subsequently regenerated by stripping it with water vapour at temperatures between 100 °C and 120 °C (TSA). The energy required for this process is inherently supplied by the power plant through waste heat, which contrasts with PSA that shows adverse practical implications due to costly compression of flue gas streams. Therefore, PSA technologies are largely limited to high-pressure gas streams in pre-combustion capture technologies. Persistent issues associated with the current amine washing process are: the large equipment, together with large amounts of solvents; the huge energy penalty of up to 40% of the power plant energy output fuel; the emission of toxic by-products; and the emission of solvents as well as their proper disposal. Estimates of the cost of effective carbon dioxide capture therefore range between US$20 and US$100 t⁻¹ and it is projected to double the present price of electricity. Conventional porous sorbents have also been extensively investigated for carbon dioxide capture, as the affinity of gas molecules for surfaces facilitates a higher capacity of a container filled with a porous material in comparison to an empty one. The main types of classical solid sorbent encompass zeolites, porous carbon and porous silica[101], all of which show considerable limitations that need to be addressed. The relatively low internal surface area of zeolites, together with their affinity for water vapour, minimizes their capacity for carbon dioxide under flue gas conditions. In contrast, activated carbons generally show very low uptakes at ambient pressure (post-combustion conditions) and are therefore suitable only for pre-combustion capture (high pressure).

the carbon dioxide problem[59]. As the carbon dioxide molecule is non-polar but has an intrinsic quadrupole moment, any moieties that are capable of inducing polarizability (for example, functional groups, open metal sites) are thus highly desirable for decorating the internal surface area of MOFs. In addition, non-polar interactions such as trapping carbon dioxide in a confined space through suitable pore sizes, or chemisorption processes with amine functionalization, are often used to boost the overall performance. Figure 4 shows a comparison of total carbon dioxide uptake (in wt%) for more than 120 MOFs with different structural features and a wide range of porosities. All of the highlighted MOFs show surface areas of roughly between 1,000 and 2,000 m² g⁻¹, suggesting a moderately high porosity to be ideal for carbon dioxide adsorption.

A material termed Mg-MOF-74 combines the features of a moderately high surface area (BET, 1,174 m² g⁻¹) with very strong open metal sites and therefore shows the highest reported carbon dioxide uptake (37.9 wt%, 1 bar) at room temperature[60]. It is isostructural to the original MOF-74 of formula $Zn_2(DOT)$ and is composed of $(Mg_3(-O)_3(-COO)_3)_\infty$ rod-like SBUs and DOT (H_4DOT, 2,5-dihydroxyterephthalic acid)[61]. Depending on the nature and strength of the open metal sites, the series of M-MOF-74 (where M is Ni,

Co, Zn and Mg) shows fundamentally different uptake capacities. A relatively high carbon dioxide uptake of 26.0 wt% was also demonstrated for Cu-TDPAT (H_6TDPAT, 2,4,6-tris(3,5-dicarboxylphenylamino)-1,3,5-triazine), a polyhedral framework with a BET surface area of 1,938 m² g⁻¹. This MOF contains both open metal sites at $Cu_2(-COO)_4$ paddlewheel SBUs and Lewis basic nitrogen moieties at the organic linkers[62]. In contrast, SIFSIX-Cu-2-i (735 m² g⁻¹) does not have open metal sites but instead it posseses polarizable SiF_6 moieties together with an interpenetrated framework that shows a narrow pore size for optimal carbon dioxide adsorption (23.8 wt%) (SIFSIX-Cu-2-i, two dimensional nets based on Cu-pyridine nodes pillared via SiF_6^{2-} anions; i, interpenetrated). In comparison, the non-interpenetrated polymorph SIFSIX-Cu-2 (3,140 m² g⁻¹) takes up less than half the amount of carbon dioxide (8.1 wt%)[63]. The introduction of amine functionalities also proved to be useful for carbon dioxide uptake, as exemplified by Zn(BTZ)[64]. The zeolitic MOF is composed of tetrahedral Zn^{2+} and BTZ (H_2BTZ, 1,5-bis(5-tetrazolo)-3-oxapentane) in a 1:1 ratio. The authors attribute the high uptake to the occurrence of multi-point interactions between carbon dioxide and the framework.

The above-mentioned materials show high uptake capacities in single-component experiments; however, the requirements of a material to perform selective carbon dioxide capture in post-combustion processes from flue gas are quite different. Aside from nitrogen as the major component (~75%), the fraction of carbon dioxide is around 15% with an additional 5–7% water. The remainder is mainly composed of oxygen, SO_x and NO_x (ref. 65). The performance assessment towards selectivity of carbon dioxide over N_2 of a particular porous material is therefore often evaluated by looking at partial pressures of carbon dioxide (0.15 bar) and N_2 (0.75 bar) without taking the water content into consideration. The comparison of selectivity is inherently difficult, as several calculation methods are currently used from single-component isotherms, through ideal adsorbed solution theory or by collecting data from column breakthrough experiments[66]. Therefore, we focus on a handful of special examples that have recently advanced to the point where it is possible to selectively capture carbon dioxide in the presence of water, a condition that should be considered in the performance of MOFs because of water's competition with carbon dioxide for the adsorptive sites[67].

Table 3 shows a selection of MOF materials that are based on two different principles for capturing carbon dioxide in the presence of water: chemisorption in the case of IRMOF-74-III-CH₂NH₂[68] and mmen-Mg_2(DOBPDC)[69], or physisorption in ZIF-300[70] and SIFSIX-3-Zn[63] (H_4DOBPDC, 4,4′-dioxido-3,3′-biphenyldicarboxylic acid; ZIF, zeolitic imidazolate framework). The capacity in wt% is calculated according to wt% = (mass of carbon dioxide)/(mass of MOF + mass of carbon dioxide) × 100%.

Chemisorption of carbon dioxide has previously been addressed in MOFs using functionalized linkers[71] or amine grafting techniques on open metal sites to facilitate capture from flue gas under dry conditions[72], in the presence of water[69], or in a cooperative manner[73]. Our group has used a different approach, by covalently bonding a highly reactive primary amine group onto an organic linker that, when combined with an infinite magnesium rod-like SBU, affords a functionalized variant of IRMOF-III[74] showing **bnn** or **etb** topology. Breakthrough experiments performed with 16% carbon dioxide and 84% nitrogen (dry, or wet with 65% relative humidity) indicate no loss of materials performance under wet conditions, as evidenced by the constant breakthrough times (Fig. 5c). This contrasts with other MOFs that rely on open metal sites for carbon dioxide capture, where the presence of water either significantly reduces their performance or is detrimental to structural preservation.

Another strategy to capture carbon dioxide relies on physisorption as demonstrated by the hydrophobic zeolitic imidazolate frameworks ZIF-300, 301 and 302. They are composed of a tetrahedral
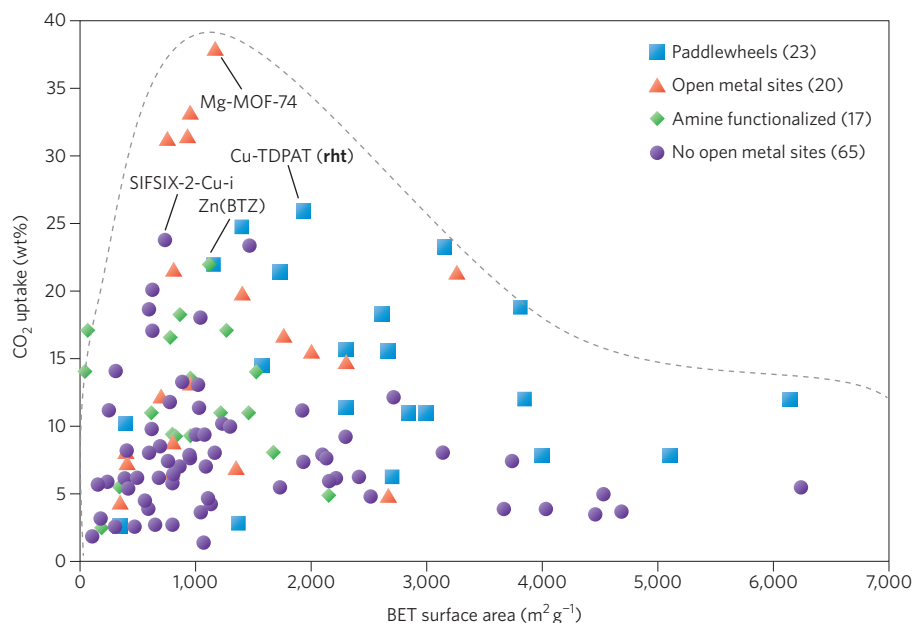
Figure 4 | Carbon dioxide uptake versus BET surface area. A total of 125 MOFs are evaluated at approximately 298 K and 1 bar. One example of each class of MOFs containing either open metal sites, paddlewheel, amine functionalized or without open metal sites is highlighted. The dotted grey line is a guide to visualize the distribution. Data used to prepare this plot and additional gas sorption properties are tabulated in Supplementary Data 1, with the corresponding references.

Table 3 | Materials showing selective carbon dioxide capture in the presence of water.

Material	Recycling method	Capacity	Sorbent type
IRMOF-74-III-CH$_2$NH$_2$[68]	Temperature swing (100 °C)	3.5 wt% (0.8 mmol g^{-1})	Chemisorption*
ZIF-300[70]	Pressure swing (room temperature)	1.4 wt% (0.3 mmol g^{-1})	Physisorption†
SIFSIX-3-Zn[63]	Pressure and temperature swing (50 °C)	9.5 wt% (2.4 mmol g^{-1})	Physisorption‡
mmen-Mg$_2$(DOBPDC)[69]	Pressure and temperature swing (100 °C)	15.6 wt% (4.2 mmol g^{-1})	Chemisorption§

*Dynamic breakthrough at 298 K, 16% (v/v) carbon dioxide, 84% (v/v) N$_2$, wet (65% relative humidity). †Dynamic breakthrough at 298 K, 16% (v/v) carbon dioxide, 84% (v/v) N$_2$, wet (80% relative humidity). ‡Column breakthrough at 298 K, 10% (v/v) carbon dioxide, 90% (v/v) N$_2$, wet (74% relative humidity). §Multicomponent adsorption at 313K, 0.11 bar carbon dioxide, 0.69 bar N$_2$, 0.02 bar H$_2$O.

Zn(Im)$_4$ (Im, imidazolate) building unit together with two types of functionalized imidazolate linker, for example, 2-mImH (2-methylimidazole) and bbImH (5(6)-bromobenzimidazole) in case of ZIF-300 (Fig. 5b) to have a chabazite (**cha**) topology. These frameworks are capable of capturing carbon dioxide under humid conditions (80% relative humidity) and show no performance loss, as evidenced by unaltered breakthrough times when compared to dry conditions (Fig. 5d). Moreover, the regeneration processes, in which carbon dioxide can be removed from the materials, are energetically favourable through purging with pure nitrogen at room temperature. This, in contrast to many other regeneration methods, some of which are mentioned in Table 3, represents a distinct advantage of such hydrophobic ZIFs in view of practical applicability, when compared with other porous materials.

Narrowing pore sizes and the introduction of polarizable inorganic anions as exemplified by Zn(PYZ)(SiF$_6$) (PYZ, pyrazine), which has later been termed SIFSIX-3-Zn[63], is another route towards high carbon dioxide affinity[63]. In this case, one-dimensional square channels that measure only 3.84 Å in diameter allow for a highly selective capture of carbon dioxide under dry and wet conditions (74% relative humidity), when exposed to a mixture of 10% carbon dioxide in nitrogen. The use of narrow-pore-size MOFs represents an ongoing, highly active research branch and is a promising strategy for carbon dioxide capture in confined space[75]. Recently, examples of MOFs have emerged that are specifically designed to contain 'single-molecule traps', offering perfectly sized pockets for carbon

dioxide. Frameworks with optimal sized polyhedra that can also be decorated with open metal sites provide a perfect fit to maximize the interaction with the carbon dioxide molecule[76].

From a practical viewpoint, MOFs for post-combustion carbon dioxide capture would need to operate under temperature swing adsorption (TSA) rather than pressure swing adsorption (PSA) conditions in a fixed-bed set-up (see Box 2). Under these conditions, the energy penalty of MOFs is considerably lower, that is, only 15–20% when compared with that of currently used monoethanolamine (MEA) solutions, due to their much lower heat capacities[77]. The heat capacity of typical MOFs (for example, Mg-MOF-74, MOF-177) ranges between 0.5 and 0.7 kJ g^{-1} K^{-1} at 25 °C, whereas a 30 wt% MEA solution (3.73 kJ g^{-1} K^{-1}) almost reaches the heat capacity of pure water (4.18 kJ g^{-1} K^{-1}). Although such heat capacities are temperature dependent, values at 25 °C provide a good estimation.

Theoretical aspects of carbon dioxide adsorption have been addressed computationally to estimate single- and mixed-component isotherms using GCMC and DFT to predict the location of carbon dioxide molecules in the pores of the framework[59]. Carbon dioxide adsorption simulations have validated experimental results and emphasize pore size rather than pore chemistry with respect to CO_2/N_2 selectivities at high pressures, that is, larger pores result in lower selectivity[78]. However, at low pressures of 0.1 atm, carbon dioxide uptake and affinity are strongly correlated with pore chemistry — for example, open metal sites — and are independent
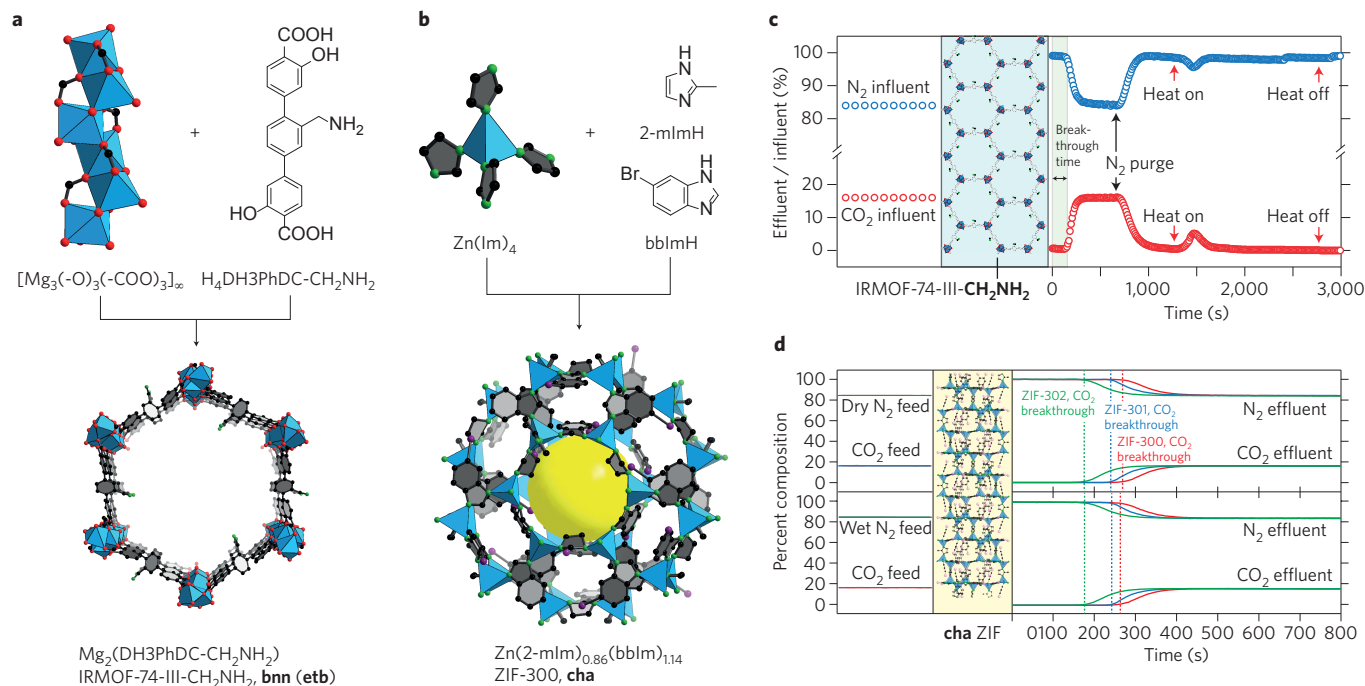
Figure 5 | Different principles of selective carbon dioxide capture in the presence of water. a, IRMOF-74-III-CH_2NH_2 is based on large channels decorated with primary amines and binds carbon dioxide through chemisorption. **b**, ZIF-300 shows pores that are decorated with hydrophobic moieties and relies on physisorption. The spheres represent the largest molecules that could fit in the pore without touching the van der Waals surface of the framework atoms. Hydrogen atoms are omitted for clarity. Colour code: black, C; red, O; green, N; purple, Br; blue, metal. $H_4DH3PhDC$-CH_2NH_2, 2′,5′-dimethyl-3,3″-dihydroxy-(1,1′:4′,1″-terphenyl)-4,4″-dicarboxylic acid; ImH, imidazole; 2-mImH, 2-methylimidazole; bbImH, 5 (6)-bromobenzimidazole. **c**, Breakthrough curves for IRMOF-74-III-CH_2NH_2. **d**, Breakthrough curves for ZIF-300. Figure reproduced with permission from: **c**, ref. 68, American Chemical Society; **d**, ref. 70, Wiley.

of pore volume or surface area[79]. As GCMC calculations require quantum mechanical calculations, charge equilibration methods have been developed to rapidly screen a larger number of MOFs for carbon dioxide capture at low pressures. These simulations agree well with experimental results and have identified a number of high-performance MOFs[80]. As mentioned above, for practical utility, water stability of some MOFs represent a challenge and has also been addressed in theoretical simulations[81]. Such simulations allow insights into dissociation mechanisms of MOFs and therefore offer solutions for the design of new stable materials.

In summary, there are critical design elements for MOFs if carbon dioxide capture applications are targeted. A surface area of roughly 1,000–2,000 $m^2 g^{-1}$ might be ideal for materials offering open metal sites and operating under dry conditions. However, in the presence of water, open metal sites are usually occupied and therefore rendered inactive, which makes the use of functional groups that can selectively bind carbon dioxide, or introduce hydrophobicity, suitable targets. Small pores also seem attractive with respect to high carbon dioxide uptake, but their capacity is inherently limited due to the relatively low surface areas. We would like to emphasize that chemisorption processes represent a promising route under flue gas conditions, given the fact that MOFs have been developed to the point where features such as high surface area and pore volume, as well as the introduction of multiple functionality, are attainable in a single material[82,83].

MOFs and related materials for carbon dioxide conversion. Carbon dioxide conversion is being studied using inorganic photocatalysts such as TiO_2 and CdS, metal impregnated zeolites and mesoporous silica[84]. As the capture of carbon dioxide has already been demonstrated in MOFs and in crystalline metallated covalent organic frameworks (COFs)[85,86], it has recently been possible to

study their use as catalysts for the conversion of carbon dioxide into high-value chemicals. Research has focused on using MOF derivatives of MIL-125(Ti), or UiO-66 and 67 (MIL, Materials Institute Lavoisier; UiO, University of Oslo), and composite materials such as HKUST-1@TiO_2 or Co-ZIF-9 with a (Ru(BPY)$_3$)Cl$_2$·6H_2O (BPY, 2,2′-bipyridine) photosensitizer[87,88].

The introduction of amino functionality into the photoactive MIL-125(Ti) afforded $Ti_8O_8(OH)_4(NH_2\text{-}BDC)_6$ (NH_2-H_2BDC, 2-amino-1,4-benzenedicarboxylic acid), termed NH_2-MIL-125(Ti). In contrast to its pristine form that shows activity only under ultraviolet irradiation (350 nm absorption edge), NH_2-MIL-125(Ti) was also demonstrated to absorb light in the visible region (550 nm), and is therefore suited to reduce carbon dioxide to HCOO$^-$ in the presence of an acetonitrile solution of triethanolamine[89]. Besides the ligand-to-metal charge transfer that modulates the absorption properties, the amino functionality also affected the overall carbon dioxide uptake capacity of NH_2-MIL-125(Ti) (132 $cm^3 g^{-1}$) in comparison to the unfunctionalized framework (99 $cm^3 g^{-1}$).

Doping of UiO-67 with (Re(CO)$_3$(DCBPY)Cl), **L** and photocatalytic linkers (H_2DCBPY, 2,2′-bipyridine-4,4′-dicarboxylic acid) gives a material of formula $Zr_6O_4(OH)_4(BPDC)_{6-x}(\textbf{L})_x$ (ref. 90). This MOF was shown to selectively reduce carbon dioxide to carbon monoxide in acetonitrile with the addition of trimethylamine as a sacrificial reagent. The turnover number was estimated to be 10.9 and therefore exceeded the molecular catalyst by having around threefold higher activity. Although the MOF showed high stability under the photocatalytic conditions, more than 40% of the Re catalyst had leached out of the framework after 20 h.

Porphyrins have also been employed as linkers to obtain materials for catalytic conversion of carbon dioxide. Combination of tetratopic or octatopic porphyrin linkers with hexagonal

$Zr_6(OH)_8(-COO)_6$ or square $Cu_2(-COO)_4$ SBUs afford PCN-224[91] and MMCF-2[92] (MMCF, metal–macrocyclic framework), respectively, which were capable of carbon dioxide fixation through carbon dioxide/epoxide coupling reactions for the production of cyclic carbonates.

Our group has recently investigated metallated COFs as heterogeneous catalysts to reduce carbon dioxide to carbon monoxide in aqueous media[93]. Two isoreticular metallated COFs, COF-366 and -367, were assembled through imine linkage of porphyrin molecular building blocks with organic struts of different length. One of the heterogeneous catalysts obtained, COF-367-Co(1%), where metal sites contain 99% Cu and 1% Co, exhibits high turnover numbers of up to 290,000 with an initial turnover frequency of 9,400 h^{-1}. This high activity of the robust and durable material represents a 26-fold enhancement in comparison to the reaction using the molecular cobalt porphyrin alone. We would also like to highlight that this reaction was carried out in water at pH 7, conditions that are economically favourable and environmentally friendly.

In the future, such porous, heterogeneous catalyst materials can play a useful role in better utilization of carbon dioxide by converting it from an unwanted by-product of energy generation into a valuable commodity, and therefore ultimately leading to a carbon-neutral energy cycle.

Outlook

The emergence of MOFs and related materials promises to advance research towards realization of a carbon-neutral energy system to a new level. The flexibility of design and synthesis of these frameworks coupled with the precision with which they can be varied and modified has already led to exceptional performance in the storage of hydrogen and methane, and the selective capture of carbon dioxide from combustion sources. Given the vast number of possible MOFs and the multiple criteria for their practical use in carbon-neutral cycle applications, we anticipate that a closer coupling between theory and experiment will continue to be fruitful in the discovery of targeted materials. Although the feasibility of using MOFs in these key applications is promising, the need for policy to drive industrial scale development will be paramount for ultimately deploying MOFs.

References

1. *BP Statistical Review of World Energy June 2015* (BP, 2015); http://go.nature.com/YgrZI1
2. *CO2 Emissions* (World Bank, 2015); http://go.nature.com/yLaqyF
3. *America's Energy Future: Technology and Transformation: Summary Edition* (National Academies Press, 2009); http://go.nature.com/YILvTAe
   This report provides information on potentials, barriers, costs and impact of energy supply and technologies.
4. Zhou, N. *et al. China's Energy and Carbon Emissions Outlook to 2050* (China Energy Group, Lawrence Berkeley National Laboratory, 2011); http://go.nature.com/toqvwR
5. *Lighting the Way: Toward a Sustainable Energy Future* (InterAcademy Council, 2007); http://go.nature.com/LfJR9g
6. *Basic Research Needs for Carbon Capture: Beyond 2020* (US Department of Energy, 2010); http://go.nature.com/1bM9qj
7. *The Impact of Increased Use of Hydrogen on Petroleum Consumption and Carbon Dioxide Emissions* (Energy Information Administration, 2008); http://go.nature.com/4Bk1jV
8. *Basic Research Needs for the Hydrogen Economy* (US Department of Energy, 2004); http://go.nature.com/GZYzy6
9. Lipman, T. *An Overview of Hydrogen Production and Storage Systems with Renewable Hydrogen Case Studies* (Clean Energy States Alliance, 2011); http://go.nature.com/p2ZuT4
10. Schlapbach, L. & Zuttel, A. Hydrogen-storage materials for mobile applications. *Nature* **414,** 353–358 (2001).
11. *Hydrogen Storage* (US Department of Energy, 2015); http://go.nature.com/ispE6Q
12. *Target Explanation Document: Onboard Hydrogen Storage for Light-Duty Fuel Cell Vehicles* (USDRIVE, 2015); http://go.nature.com/EHHdZ5
13. Zoellter, J. Mercedes-Benz F125 concept: Mercedes' dream of a 2025 S-class takes flight. *Car and Driver* (21 October 2015); http://go.nature.com/kFaC3e
14. Sudik, A. *et al. Ford/BASF-SE/UM Activities in Support of the Hydrogen Storage Engineering Center of Excellence* (HSECoE, 2015); http://go.nature.com/SrJePp
15. Wang, X.-S. *et al.* Enhancing H$_2$ uptake by "close-packing" alignment of open copper sites in metal–organic frameworks. *Angew. Chem. Int. Ed.* **47,** 7263–7266 (2008).
16. Suh, M. P., Park, H. J., Prasad, T. K. & Lim, D.-W. Hydrogen storage in metal–organic frameworks. *Chem. Rev.* **112,** 782–835 (2012).
17. Rowsell, J. L. C. & Yaghi, O. M. Effects of functionalization, catenation, and variation of the metal oxide and organic linking units on the low-pressure hydrogen adsorption properties of metal–organic frameworks. *J. Am. Chem. Soc.* **128,** 1304–1315 (2006).
18. Rowsell, J. L. C. & Yaghi, O. M. Strategies for hydrogen storage in metal–organic frameworks. *Angew. Chem. Int. Ed.* **44,** 4670–4679 (2005).
    This paper highlights different strategies for hydrogen storage in MOFs being used today and has led to room temperature uptake of 2–3 wt% and 6 wt% at 77 K.
19. Mulfort, K. L., Farha, O. K., Stern, C. L., Sarjeant, A. A. & Hupp, J. T. Post-synthesis alkoxide formation within metal–organic framework materials: a strategy for incorporating highly coordinatively unsaturated metal ions. *J. Am. Chem. Soc.* **131,** 3866–3868 (2009).
20. Li, Y. & Yang, R. T. Significantly enhanced hydrogen storage in metal–organic frameworks via spillover. *J. Am. Chem. Soc.* **128,** 726–727 (2006).
21. Chae, H. K. *et al.* A route to high surface area, porosity and inclusion of large molecules in crystals. *Nature* **427,** 523–527 (2004).
    This contribution details a strategy and interpretation for using exposed six-membered rings to make ultrahigh-porosity MOFs.
22. Furukawa, H., Miller, M. A. & Yaghi, O. M. Independent verification of the saturation hydrogen uptake in MOF-177 and establishment of a benchmark for hydrogen adsorption in metal–organic frameworks. *J. Mater. Chem.* **17,** 3197–3204 (2007).
23. Carlucci, L., Ciani, G. & Proserpio, D. M. Polycatenation, polythreading and polyknotting in coordination network chemistry. *Coord. Chem. Rev.* **246,** 247–289 (2003).
24. Furukawa, H. *et al.* Ultrahigh porosity in metal–organic frameworks. *Science* **329,** 424–428 (2010).
25. Grunker, R. *et al.* A new metal–organic framework with ultra-high surface area. *Chem. Commun.* **50,** 3450–3452 (2014).
26. Eddaoudi, M. *et al.* Porous metal–organic polyhedra: 25 Å cuboctahedron constructed from 12 Cu$_2$(CO$_2$)$_4$ paddle-wheel building blocks. *J. Am. Chem. Soc.* **123,** 4368–4369 (2001).
27. Moulton, B., Lu, J., Mondal, A. & Zaworotko, M. J. Nanoballs: nanoscale faceted polyhedra with large windows and cavities. *Chem. Commun.* **9,** 863–864 (2001).
28. Nouar, F. *et al.* Supermolecular building blocks (SBBs) for the design and synthesis of highly porous metal–organic frameworks. *J. Am. Chem. Soc.* **130,** 1833–1835 (2008).
    This contribution provided the foundation for a large class of isoreticular MOFs with high H$_2$ adsorption.
29. Yan, Y. *et al.* Metal–organic polyhedral frameworks: high H$_2$ adsorption capacities and neutron powder diffraction studies. *J. Am. Chem. Soc.* **132,** 4092–4094 (2010).
30. Yuan, D., Zhao, D., Sun, D. & Zhou, H.-C. An isoreticular series of metal–organic frameworks with dendritic hexacarboxylate ligands and exceptionally high gas-uptake capacity. *Angew. Chem. Int. Ed.* **49,** 5357–5361 (2010).
31. Farha, O. K. *et al. De novo* synthesis of a metal–organic framework material featuring ultrahigh surface area and gas storage capacities. *Nature Chem.* **2,** 944–948 (2010).
32. Farha, O. K. *et al.* Designing higher surface area metal–organic frameworks: are triple bonds better than phenyls? *J. Am. Chem. Soc.* **134,** 9860–9863 (2012).
33. Farha, O. K. *et al.* Metal–organic framework materials with ultrahigh surface areas: is the sky the limit? *J. Am. Chem. Soc.* **134,** 15016–15021 (2012).
    This paper reports a MOF that currently holds the world record with respect to BET surface area.
34. Liu, L., Konstas, K., Hill, M. R. & Telfer, S. G. Programmed pore architectures in modular quaternary metal–organic frameworks. *J. Am. Chem. Soc.* **135,** 17731–17734 (2013).
35. Schoedel, A., Boyette, W., Wojtas, L., Eddaoudi, M. & Zaworotko, M. J. A family of porous lonsdaleite-e networks obtained through pillaring of decorated kagomé lattice sheets. *J. Am. Chem. Soc.* **135,** 14016–14019 (2013).
36. Schoedel, A. *et al.* The asc trinodal platform: two-step assembly of triangular, tetrahedral, and trigonal-prismatic molecular building blocks. *Angew. Chem. Int. Ed.* **52,** 2902–2905 (2013).

37. Frost, H., Düren, T. & Snurr, R. Q. Effects of surface area, free volume, and heat of adsorption on hydrogen uptake in metal–organic frameworks. *J. Phys. Chem. B* **110,** 9565–9570 (2006).

38. Yang, Q. & Zhong, C. Understanding hydrogen adsorption in metal–organic frameworks with open metal sites: a computational study. *J. Phys. Chem. B* **110,** 655–658 (2006).

39. Cheon, Y. E., Park, J. & Suh, M. P. Selective gas adsorption in a magnesium-based metal–organic framework. *Chem. Commun.* **36,** 5436–5438 (2009).

40. Bae, Y.-S. & Snurr, R. Q. Optimal isosteric heat of adsorption for hydrogen storage and delivery using metal–organic frameworks. *Micropor. Mesopor. Mater.* **132,** 300–303 (2010).

41. Ren, J., Langmi, H. W., North, B. C. & Mathe, M. Review on processing of metal–organic framework (MOF) materials towards system integration for hydrogen storage. *Int. J. Energy Res.* **39,** 607–620 (2015).

42. *MOVE Program Overview* (ARPA-E, 2012); http://go.nature.com/Vuqhoi

43. Peng, Y. *et al.* Methane storage in metal–organic frameworks: current records, surprise findings, and challenges. *J. Am. Chem. Soc.* **135,** 11887–11894 (2013).

44. Simon, C. M. *et al.* The materials genome in action: identifying the performance limits for methane storage. *Energy Environ. Sci.* **8,** 1190–1199 (2015).

45. Eddaoudi, M. *et al.* Systematic design of pore size and functionality in isoreticular MOFs and their application in methane storage. *Science* **295,** 469–472 (2002).
   This publication describes use of the isoreticular principle in making MOFs and designing their interior for methane storage.

46. Li, H., Eddaoudi, M., O'Keeffe, M. & Yaghi, O. M. Design and synthesis of an exceptionally stable and highly porous metal–organic framework. *Nature* **402,** 276–279 (1999).
   This contribution revealed the first MOF with porosity and surface area exceeding previous records, and featuring a robust architecture.

47. Noro, S.-i., Kitagawa, S., Kondo, M. & Seki, K. A new, methane adsorbent, porous coordination polymer [{CuSiF₆(4,4′-bipyridine)₂}ₙ]. *Angew. Chem. Int. Ed.* **39,** 2081–2084 (2000).

48. Chui, S. S. Y., Lo, S. M. F., Charmant, J. P. H., Orpen, A. G. & Williams, I. D. A chemically functionalizable nanoporous material [Cu₃(TMA)₂(H₂O)₃]ₙ. *Science* **283,** 1148–1150 (1999).

49. Gándara, F., Furukawa, H., Lee, S. & Yaghi, O. M. High methane storage capacity in aluminum metal–organic frameworks. *J. Am. Chem. Soc.* **136,** 5271–5274 (2014).
   This paper shows that the availability of terminal polyphenylene units as terminal ligands in MOFs provides for ultrahigh methane delivery.

50. Alezi, D. *et al.* MOF crystal chemistry paving the way to gas storage needs: aluminum-based soc-MOF for CH₄, O₂, and CO₂ storage. *J. Am. Chem. Soc.* **137,** 13308–13318 (2015).

51. Wilmer, C. E. *et al.* Gram-scale, high-yield synthesis of a robust metal–organic framework for storing methane and other gases. *Energy Environ. Sci.* **6,** 1158–1163 (2013).

52. Wu, H., Zhou, W. & Yildirim, T. High-capacity methane storage in metal–organic frameworks M₂(dhtp): the important role of open metal sites. *J. Am. Chem. Soc.* **131,** 4995–5000 (2009).

53. Wilmer, C. E. *et al.* Large-scale screening of hypothetical metal–organic frameworks. *Nature Chem.* **4,** 83–89 (2012).

54. Luthi, D. *et al.* High-resolution carbon dioxide concentration record 650,000–800,000 years before present. *Nature* **453,** 379–382 (2008).

55. *Atmospheric CO₂ Data* (Scripps Institution of Oceanography, 2015); http://go.nature.com/z3Cgf5

56. Socolow, R. *Stabilization Wedges and the Polygame* (2013); http://go.nature.com/7j8mBi

57. Pacala, S. & Socolow, R. Stabilization wedges: solving the climate problem for the next 50 years with current technologies. *Science* **305,** 968–972 (2004).

58. Orr, J. F. M. CO₂ capture and storage: are we ready? *Energy Environ. Sci.* **2,** 449–458 (2009).

59. Sumida, K. *et al.* Carbon dioxide capture in metal–organic frameworks. *Chem. Rev.* **112,** 724–781 (2012).

60. Caskey, S. R., Wong-Foy, A. G. & Matzger, A. J. Dramatic tuning of carbon dioxide uptake via metal substitution in a coordination polymer with cylindrical pores. *J. Am. Chem. Soc.* **130,** 10870–10871 (2008).

61. Rosi, N. L. *et al.* Rod packings and metal–organic frameworks constructed from rod-shaped secondary building units. *J. Am. Chem. Soc.* **127,** 1504–1518 (2005).

62. Li, B. *et al.* Enhanced binding affinity, remarkable selectivity, and high capacity of CO₂ by dual functionalization of a rht-type metal–organic framework. *Angew. Chem. Int. Ed.* **51,** 1412–1415 (2012).

63. Nugent, P. *et al.* Porous materials with optimal adsorption thermodynamics and kinetics for CO₂ separation. *Nature* **495,** 80–84 (2013).
   This publication shows a crystal engineering strategy to control pore funtionality and size in MOFs for CO₂ separation in the presence of water.

64. Cui, P. *et al.* Multipoint interactions enhanced CO₂ uptake: a zeolite-like zinc–tetrazole framework with 24-nuclear zinc cages. *J. Am. Chem. Soc.* **134,** 18892–18895 (2012).

65. Granite, E. J. & Pennline, H. W. Photochemical removal of mercury from flue gas. *Ind. Eng. Chem. Res.* **41,** 5470–5476 (2002).

66. Britt, D., Furukawa, H., Wang, B., Glover, T. G. & Yaghi, O. M. From the cover: highly efficient separation of carbon dioxide by a metal–organic framework replete with open metal sites. *Proc. Natl Acad. Sci. USA* **106,** 20637–20640 (2009).

67. Liu, J., Thallapally, P. K., McGrail, B. P., Brown, D. R. & Liu, J. Progress in adsorption-based CO₂ capture by metal–organic frameworks. *Chem. Soc. Rev.* **41,** 2308–2322 (2012).

68. Fracaroli, A. M. *et al.* Metal–organic frameworks with precisely designed interior for carbon dioxide capture in the presence of water. *J. Am. Chem. Soc.* **136,** 8863–8866 (2014).
   This paper demonstrates a method for covalently functionalizing the interior of MOFs to capture CO₂ in the presence of water.

69. Mason, J. A. *et al.* Application of a high-throughput analyzer in evaluating solid adsorbents for post-combustion carbon capture via multicomponent adsorption of CO₂, N₂, and H₂O. *J. Am. Chem. Soc.* **137,** 4787–4803 (2015).

70. Nguyen, N. T. *et al.* Selective capture of carbon dioxide under humid conditions by hydrophobic chabazite-type zeolitic imidazolate frameworks. *Angew. Chem. Int. Ed.* **53,** 10645–10648 (2014).

71. Vaidhyanathan, R. *et al.* Direct observation and quantification of CO₂ binding within an amine-functionalized nanoporous solid. *Science* **330,** 650–653 (2010).

72. McDonald, T. M. *et al.* Capture of carbon dioxide from air and flue gas in the alkylamine-appended metal–organic framework mmen-Mg2(dobpdc). *J. Am. Chem. Soc.* **134,** 7056–7065 (2012).

73. McDonald, T. M. *et al.* Cooperative insertion of CO₂ in diamine-appended metal–organic frameworks. *Nature* **519,** 303–308 (2015).

74. Deng, H. *et al.* Large-pore apertures in a series of metal–organic frameworks. *Science* **336,** 1018–1023 (2012).

75. Xiang, S. *et al.* Microporous metal–organic framework with potential for carbon dioxide capture at ambient conditions. *Nature Commun.* **3,** 954 (2012).

76. Li, J.-R. *et al.* Porous materials with pre-designed single-molecule traps for CO₂ selective adsorption. *Nature Commun.* **4,** 1538 (2013).

77. Mason, J. A., Sumida, K., Herm, Z. R., Krishna, R. & Long, J. R. Evaluating metal–organic frameworks for post-combustion carbon dioxide capture via temperature swing adsorption. *Energy Environ. Sci.* **4,** 3030–3040 (2011).

78. Liu, B. & Smit, B. Comparative molecular simulation study of CO₂/N₂ and CH₄/N₂ Separation in zeolites and metal–organic frameworks. *Langmuir* **25,** 5918–5926 (2009).

79. Yazaydın, A. O. *et al.* Screening of metal–organic frameworks for carbon dioxide capture from flue gas using a combined experimental and modeling approach. *J. Am. Chem. Soc.* **131,** 18198–18199 (2009).

80. Wilmer, C. E. & Snurr, R. Q. Towards rapid computational screening of metal–organic frameworks for carbon dioxide capture: calculation of framework charges via charge equilibration. *Chem. Eng. J.* **171,** 775–781 (2011).

81. Greathouse, J. A. & Allendorf, M. D. The interaction of water with MOF-5 simulated by molecular dynamics. *J. Am. Chem. Soc.* **128,** 10678–10679 (2006).

82. Deng, H. *et al.* Multiple functional groups of varying ratios in metal–organic frameworks. *Science* **327,** 846–850 (2010).

83. Furukawa, H., Müller, U. & Yaghi, O. M. "Heterogeneity within order" in metal–organic frameworks. *Angew. Chem. Int. Ed.* **54,** 3417–3430 (2015).

84. Somorjai, G. A., Frei, H. & Park, J. Y. Advancing the frontiers in nanocatalysis, biointerfaces, and renewable energy conversion by innovations of surface techniques. *J. Am. Chem. Soc.* **131,** 16589–16605 (2009).

85. Côté, A. P. *et al.* Porous, crystalline, covalent organic frameworks. *Science* **310,** 1166–1170 (2005).

86. Furukawa, H. & Yaghi, O. M. Storage of hydrogen, methane, and carbon dioxide in highly porous covalent organic frameworks for clean energy applications. *J. Am. Chem. Soc.* **131,** 8875–8883 (2009).

87. Zhang, T. & Lin, W. Metal–organic frameworks for artificial photosynthesis and photocatalysis. *Chem. Soc. Rev.* **43,** 5982–5993 (2014).

88. Wang, C.-C., Zhang, Y.-Q., Li, J. & Wang, P. Photocatalytic CO₂ reduction in metal–organic frameworks: a mini review. *J. Mol. Struct.* **1083,** 127–136 (2015).

89. Fu, Y. *et al.* An amine-functionalized titanium metal–organic framework photocatalyst with visible-light-induced activity for CO₂ reduction. *Angew. Chem. Int. Ed.* **51,** 3364–3367 (2012).

90. Wang, C., Xie, Z., deKrafft, K. E. & Lin, W. Doping metal–organic frameworks for water oxidation, carbon dioxide reduction, and organic photocatalysis. *J. Am. Chem. Soc.* **133,** 13445–13454 (2011).

91. Feng, D. *et al.* Construction of ultrastable porphyrin Zr metal–organic frameworks through linker elimination. *J. Am. Chem. Soc.* **135,** 17105–17110 (2013).

92. Gao, W.-Y. *et al.* Crystal engineering of an nbo topology metal–organic framework for chemical fixation of CO_2 under ambient conditions. *Angew. Chem. Int. Ed.* **53,** 2615–2619 (2014).

93. Lin, S. *et al.* Covalent organic frameworks comprising cobalt porphyrins for catalytic CO_2 reduction in water. *Science* **349,** 1208–1213 (2015).

94. Park, H. J., Lim, D.-W., Yang, W. S., Oh, T.-R. & Suh, M. P. A highly porous metal–organic framework: structural transformations of a guest-free MOF depending on activation method and temperature. *Chem. Eur. J.* **17,** 7251–7260 (2011).

95. Yaghi, O. M. *et al.* Reticular synthesis and the design of new materials. *Nature* **423,** 705–714 (2003).

96. Eddaoudi, M. *et al.* Modular chemistry: secondary building units as a basis for the design of highly porous and robust metal–organic carboxylate frameworks. *Acc. Chem. Res.* **34,** 319–330 (2001).

97. Furukawa, H., Cordova, K. E., O'Keeffe, M. & Yaghi, O. M. The chemistry and applications of metal–organic frameworks. *Science* **341,** 1230444 (2013).

98. Yaghi, O. M., Li, G. & Li, H. Selective binding and removal of guests in a microporous metal–organic framework. *Nature* **378,** 703–706 (1995).

99. Rochelle, G. T. Amine scrubbing for CO_2 capture. *Science* **325,** 1652–1654 (2009).

100. Haszeldine, R. S. Carbon capture and storage: how green can black be? *Science* **325,** 1647–1652 (2009).

101. Siriwardane, R. V., Shen, M.-S., Fisher, E. P. & Poston, J. A. Adsorption of CO_2 on molecular sieves and activated carbon. *Energy Fuels* **15,** 279–284 (2001).

Additional information

Supplementary information is available online. Reprints and permissions information is available online at www.nature.com/reprints. Correspondence should be addressed to O.M.Y.

Competing interests

The authors declare no competing financial interests.